Supplementary Information (SI) for Journal of Materials Chemistry A.

Graphene Oxide Dough Composites: Direct Mixing and Structural Design Strategies for High-performance Electronics and Energy Applications

Authors: Seoyeon Park[a,b], Jeonghyun Yoo[a], Kyeong Ja Kim[c], Soong Ju Oh[b], Byung-Su Kim [a,], and Ji-Hyuk Choi[a,*]*

[a]Resources & Materials Research Center, Korea Institute of Geoscience and Mineral Resources, Daejeon, 34132, Republic of Korea

[b]Department of Materials Science and Engineering, Korea University, 145, Anam-ro Seongbuk-gu, Seoul, 02841, Republic of Korea

[c]Space Resources Exploration and Utilization Center, Korea Institute of Geoscience and Mineral Resources, Daejeon, 34132, Republic of Korea

* Corresponding author

E-mail addresses: bskim@kigam.re.kr, jhcho@kigam.re.kr

(a)

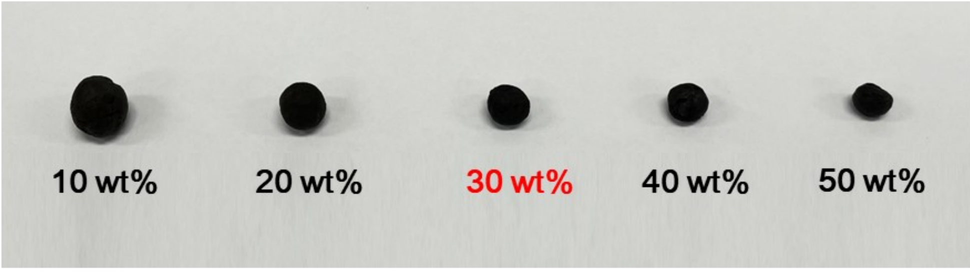

(b)

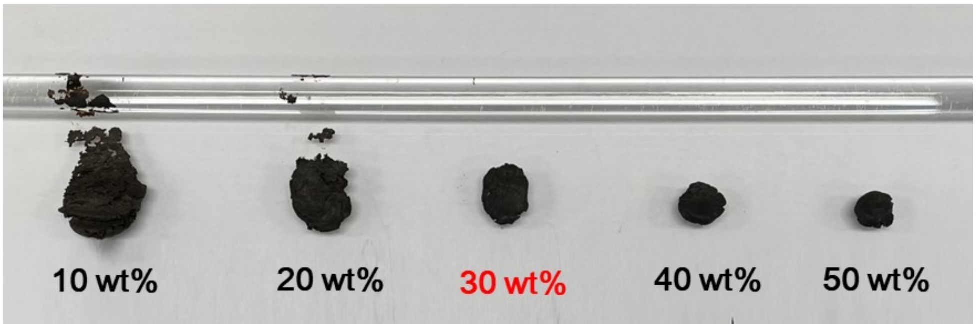

Figure S1. (a) The appearance of GODs with different wt% of GO content using ethanol as a solvent, and (b) when they were pushed with a glass rod.

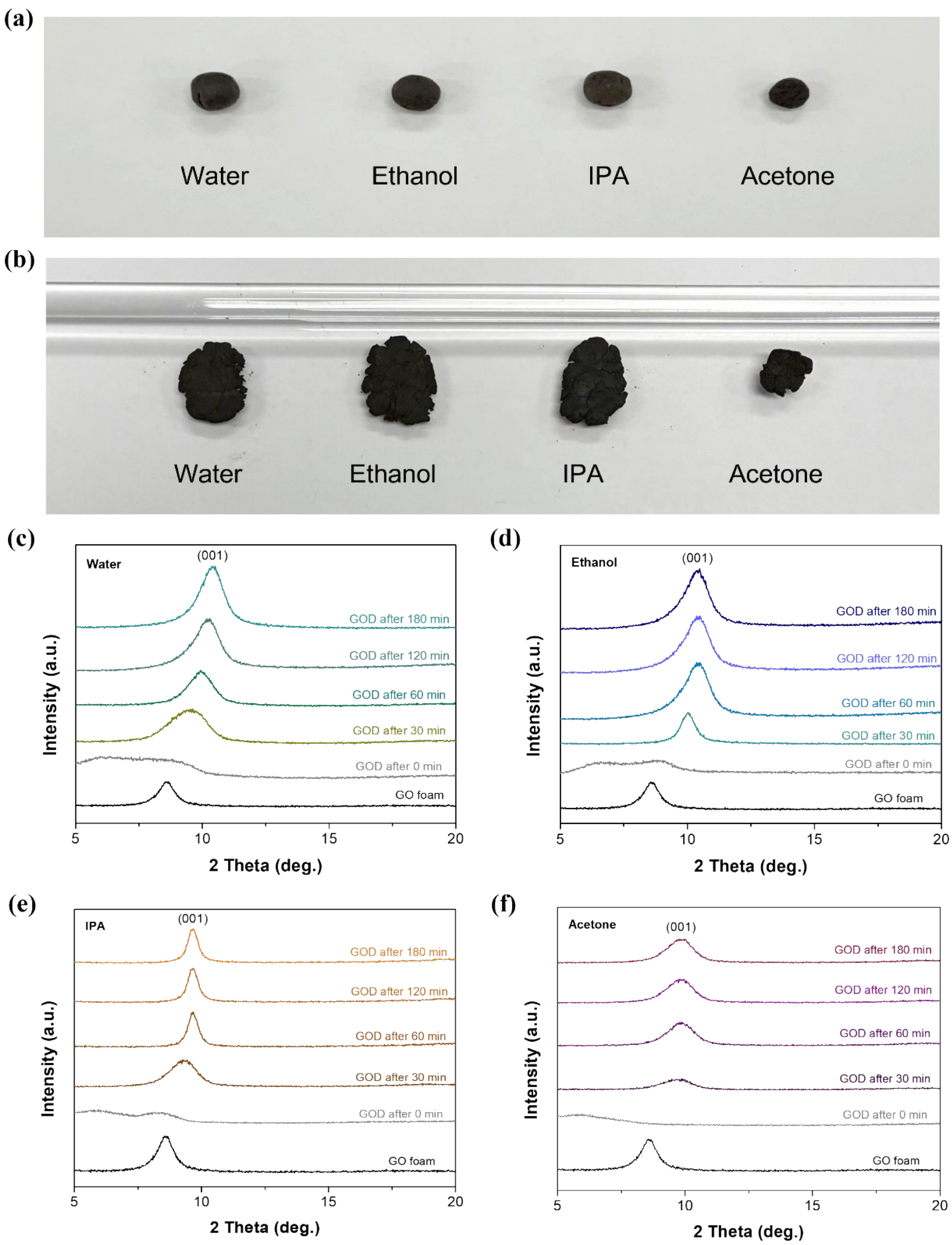

Figure S2. (a) Formation of GODs using different polar solvents, and (b) their deformation response when pressed with a glass rod. (c-f) XRD patterns of GODs prepared with different polar solvents under varying exposure times in ambient conditions.

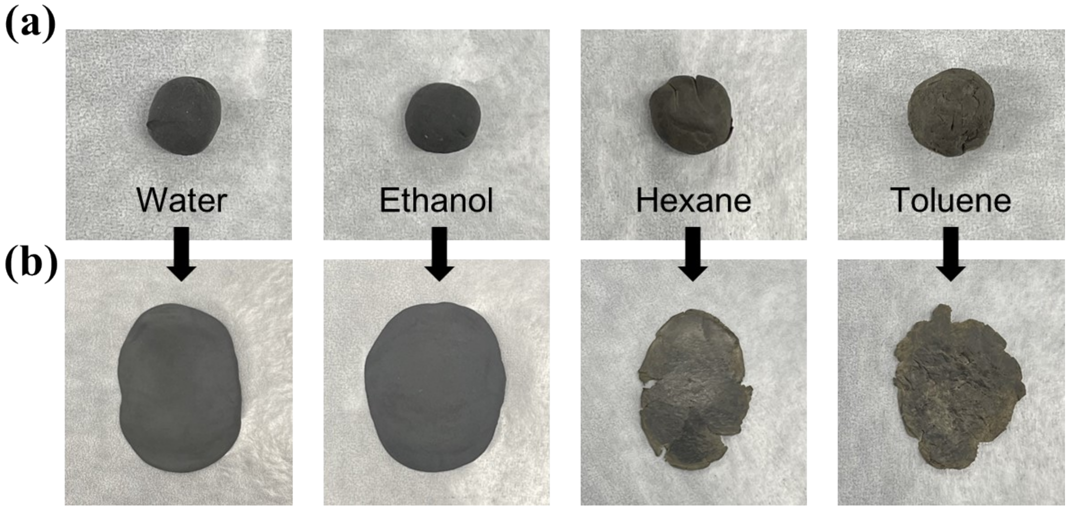

Figure S3. (a) Images of GOD formation (30 wt% of GO content) using polar solvents (water and ethanol) and non-polar solvents (hexane and toluene), and (b) fabricated films of the GODs.

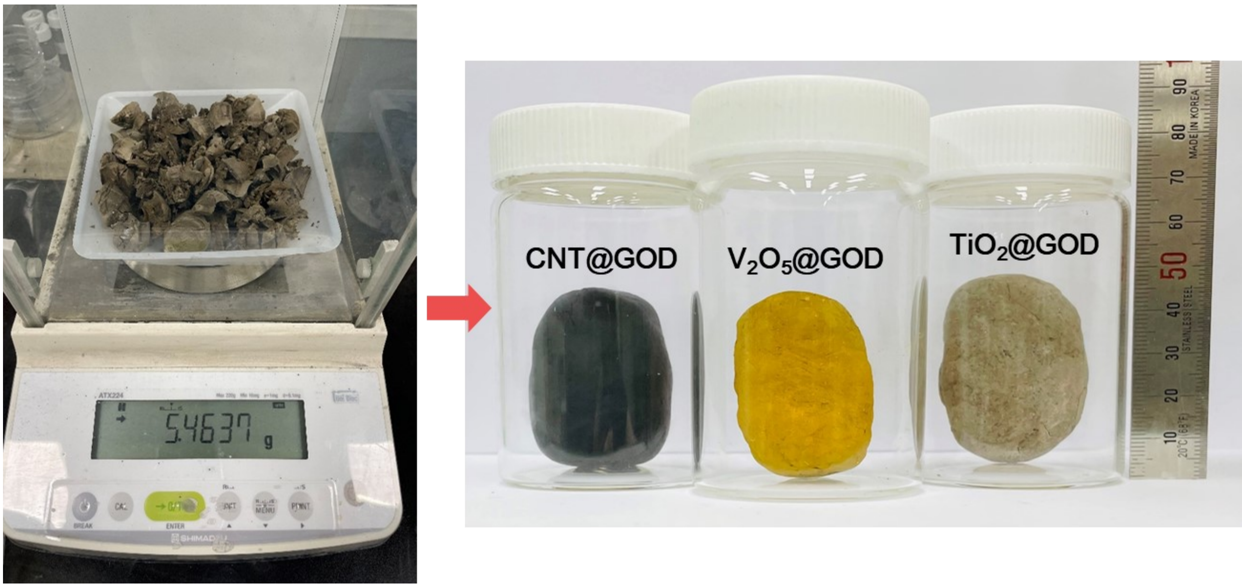

Figure S4. Photos showing the amount of GO foams for a large-scale production of GOD composites, and when they were fabricated into CNT@GOD, V_2O_5@GOD, and TiO_2@GOD at a large-scale.

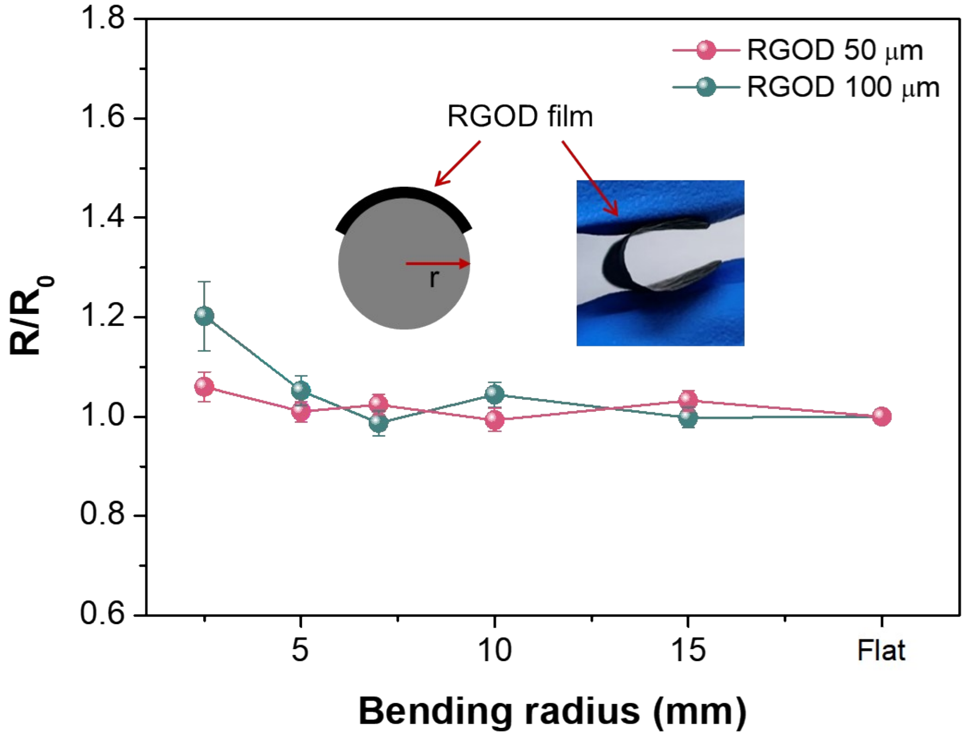

Figure S5. Relative resistance changes according to bending radii (2.5, 5, 7, 10 and 15 mm) for RGOD films with thicknesses of 50 μm and 100 μm

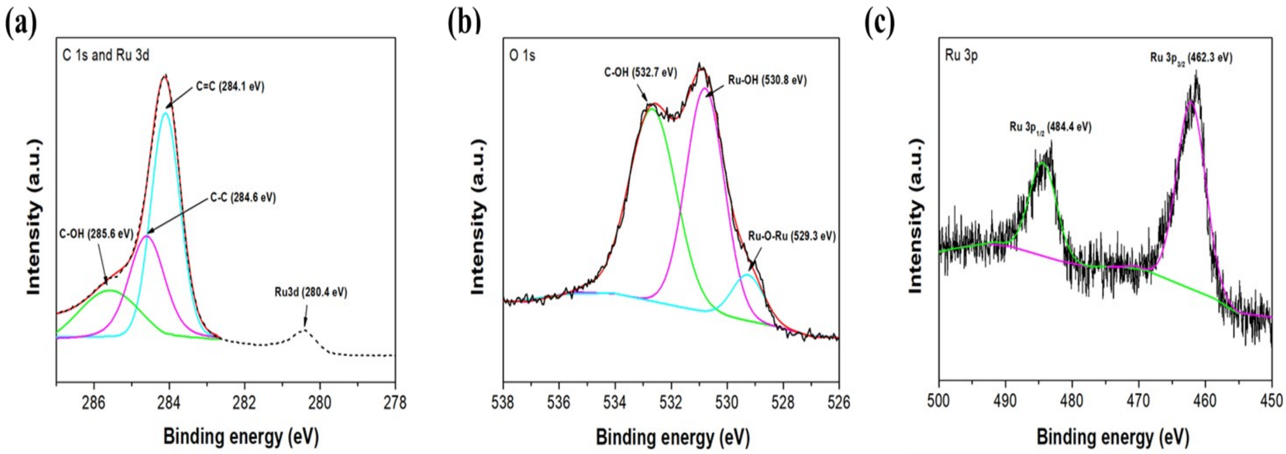

Figure S6. The XPS spectra of RuO_2@RGOD of (a) C 1s and R 3d, (b) O 1s, and (c) Ru 3p.

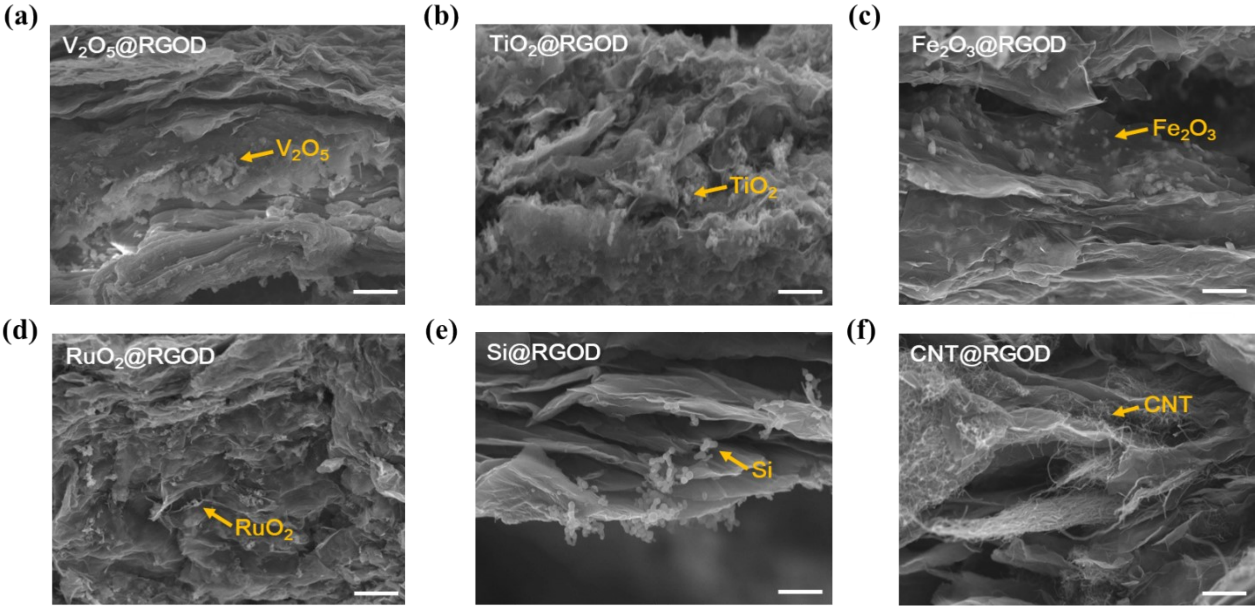

Figure S7. The **c**ross-sectional SEM images of RGOD composites mixed with (a) V_2O_5, (b) TiO_2, (c) Fe_2O_3, (d) RuO_2, (e) Si nanoparticles, and (f) CNTs. (scale bar: 500 nm)

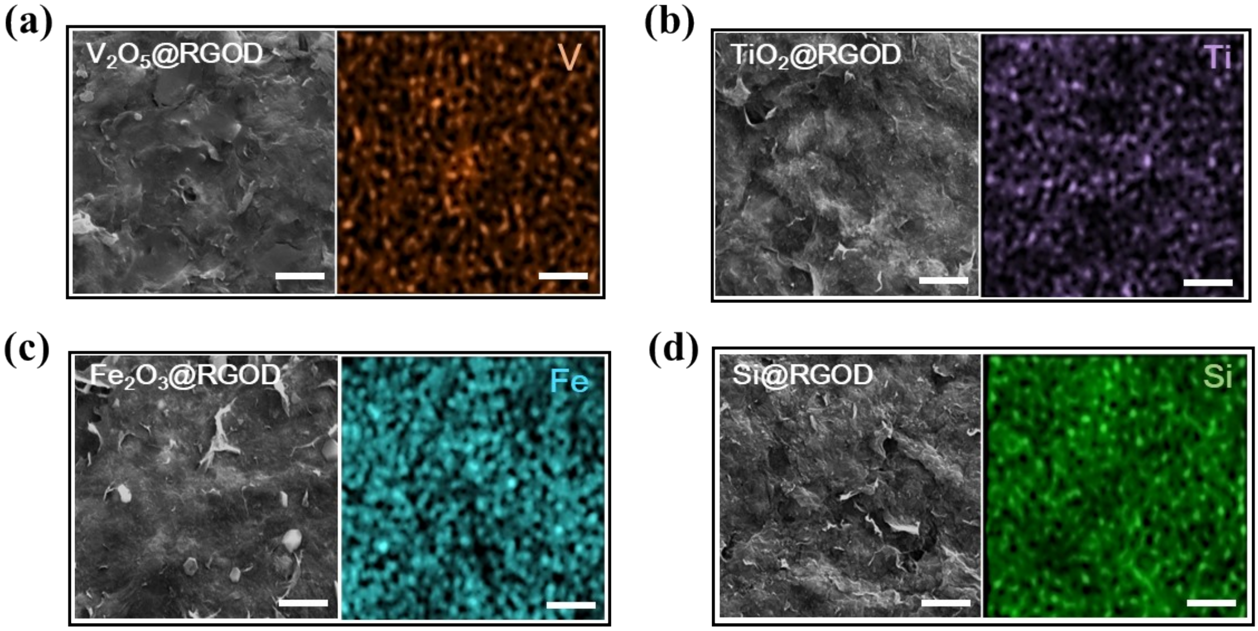

Figure S8. The SEM surface images and their EDS mapping images of the RGOD composites mixed with (a) V_2O_5, (b) TiO_2, (c) Fe_2O_3, and (d) Si nanoparticles. (scale bar: 2 μm)

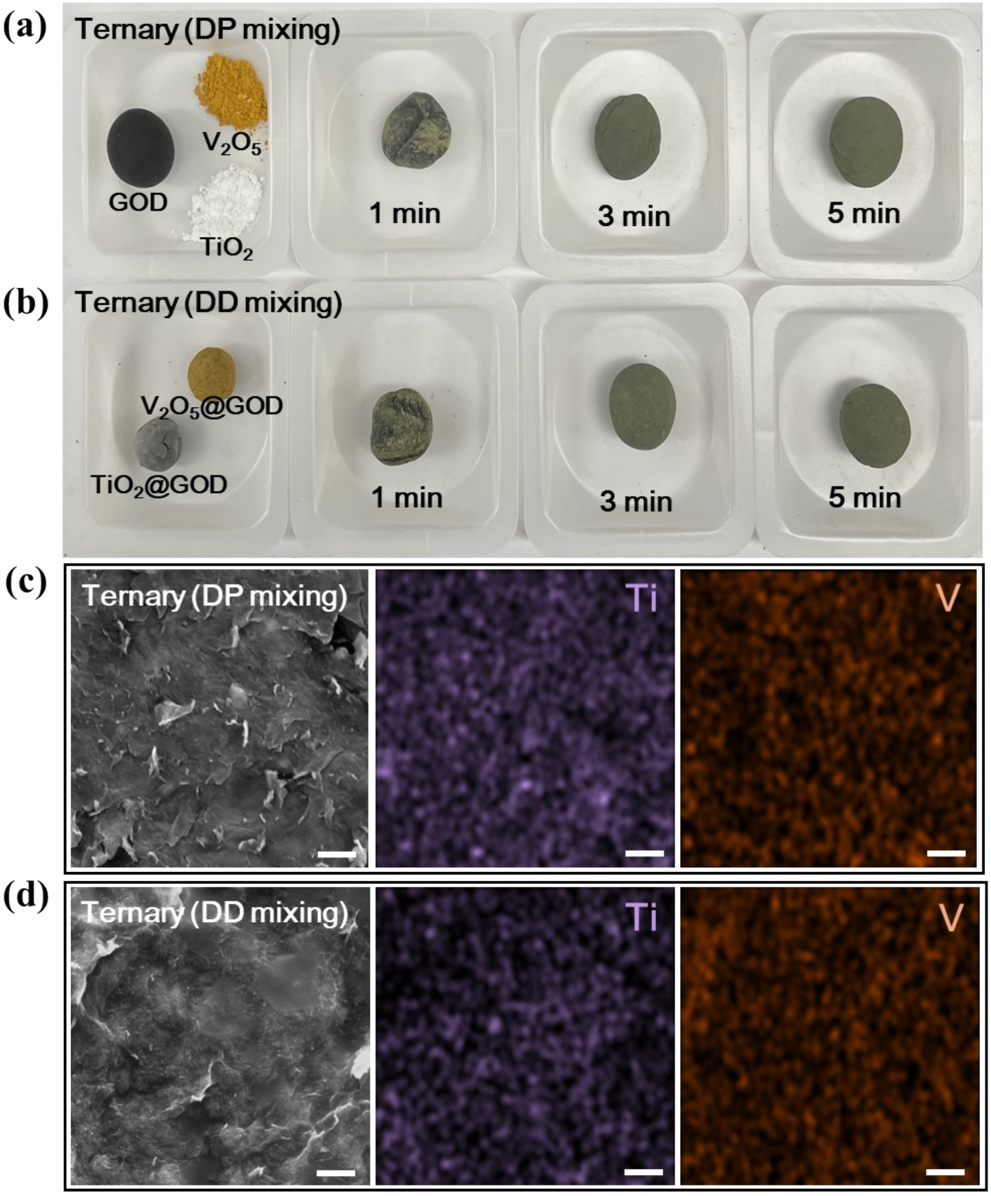

Figure S9. (a-b) Photos taken before and after mixing ternary GOD composites ($TiO_2@V_2O_5@GOD$) depending on processing time using an acoustic mixer. (c-d) SEM surface images and corresponding EDS mapping images of the ternary GOD composites fabricated by DD and DP mixing. (scale bar: 2 μm).

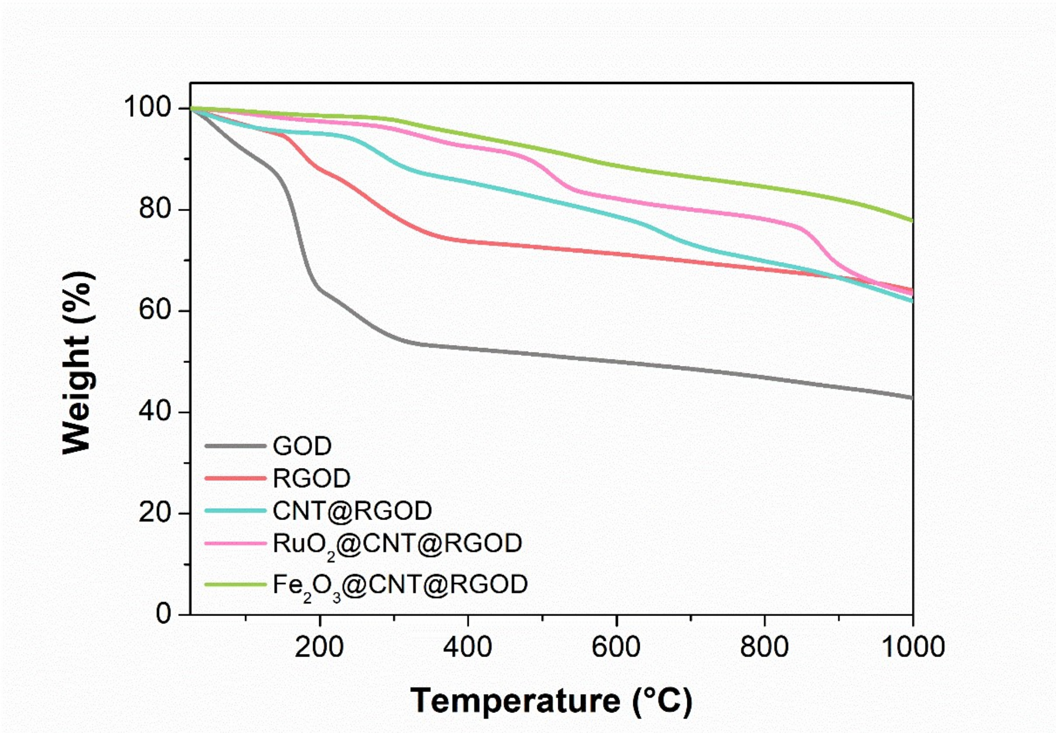

Figure S10. The TGA curves of GOD, RGOD, and RGOD composites including CNT@RGOD, RuO_2@CNT@RGOD, and Fe_2O_3@CNT@RGOD.

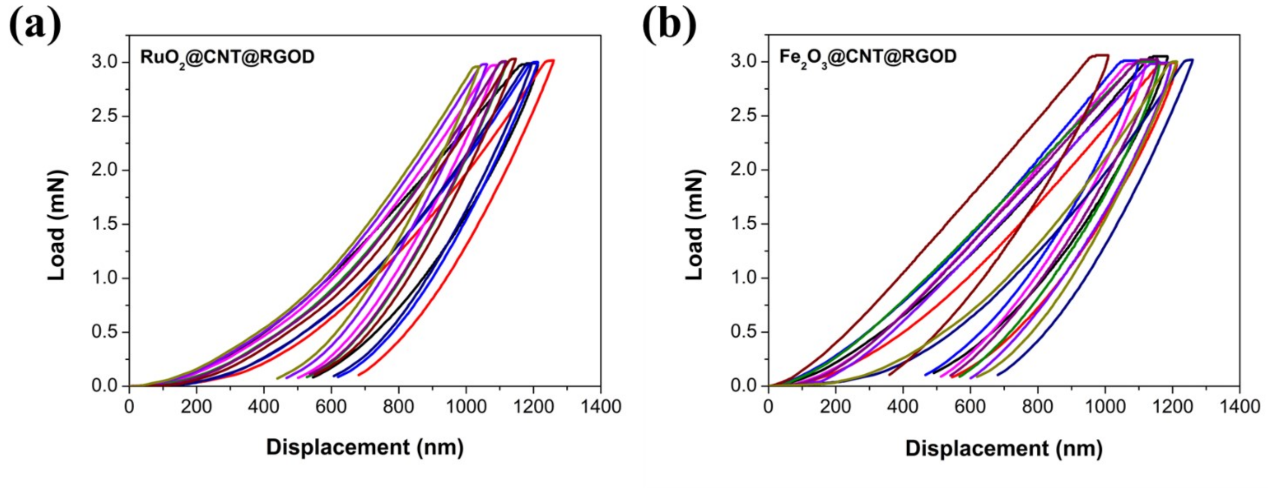

Figure S11. Cyclic load–displacement curves under a constant load of 3 mN for RGOD composites of (a) RuO_2@CNT@RGOD and (b) Fe_2O_3@CNT@RGOD.

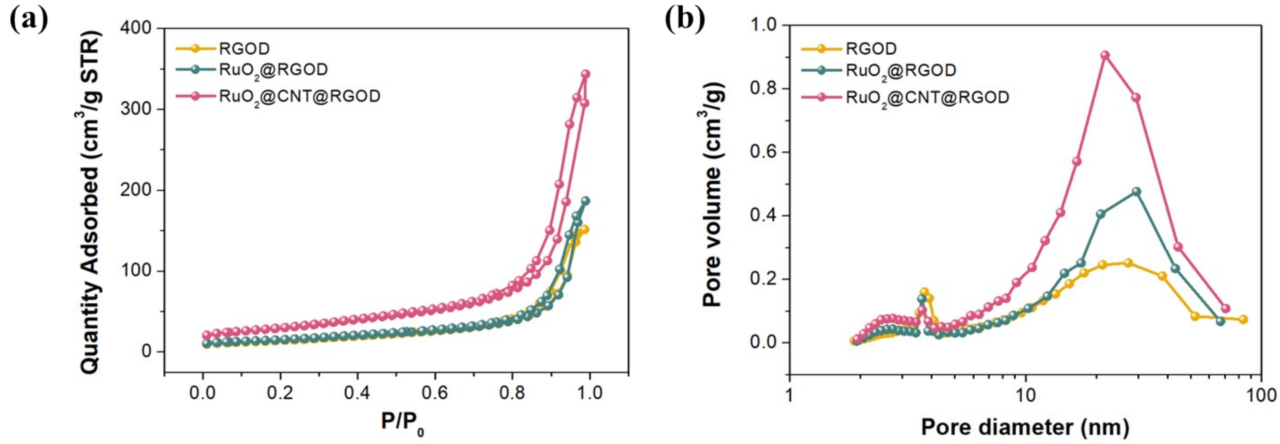

Figure S12. (a) BET adsorption-desorption curves and (b) pore volume distributions of RGOD, RuO_2@RGOD and RuO_2@CNT@RGOD films.

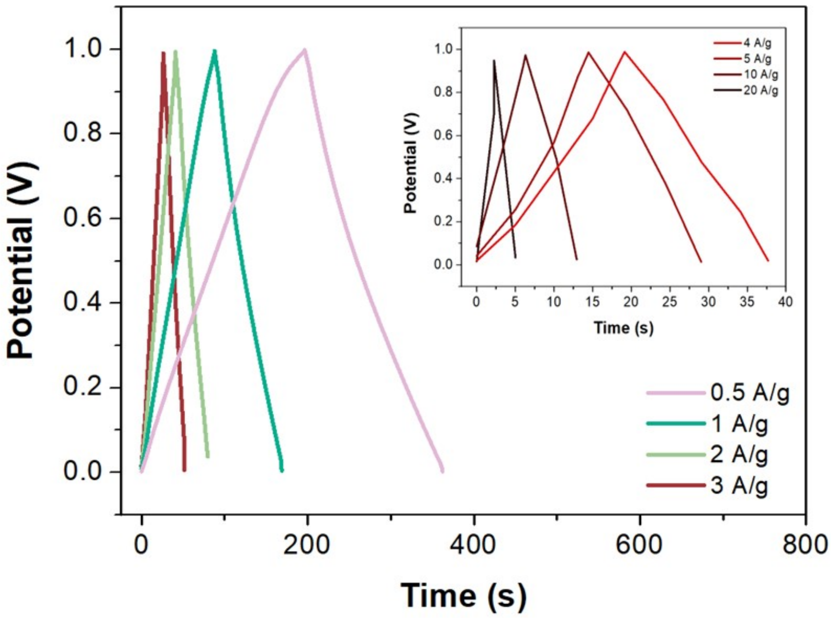

Figure S13. GCD curves of RuO_2@CNT@RGOD film at different current densities.

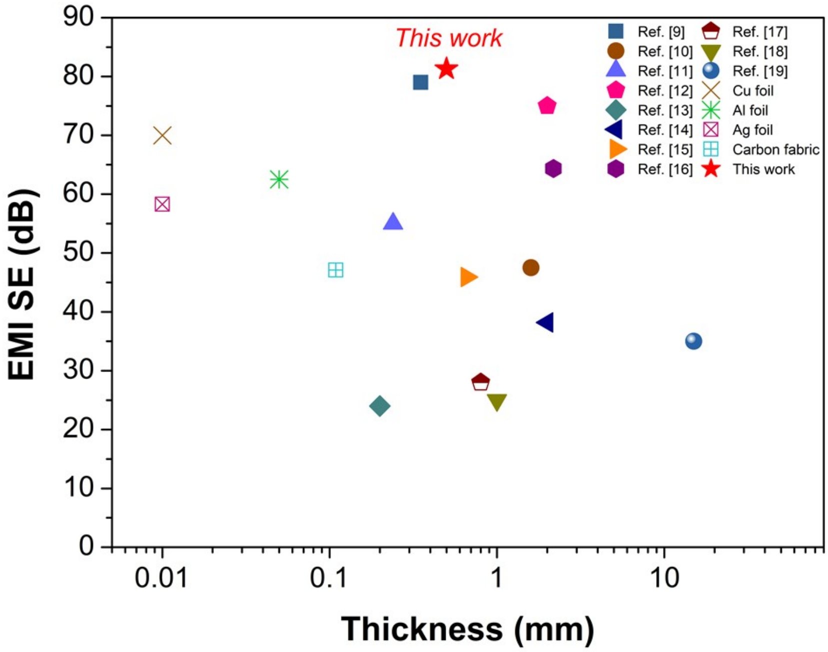

Figure S14. Comparison of EMI shielding performance of Fe_2O_3@CNT@RGOD as a function of thickness, along with various polymer-free graphene composite materials and representative commercial shielding materials.

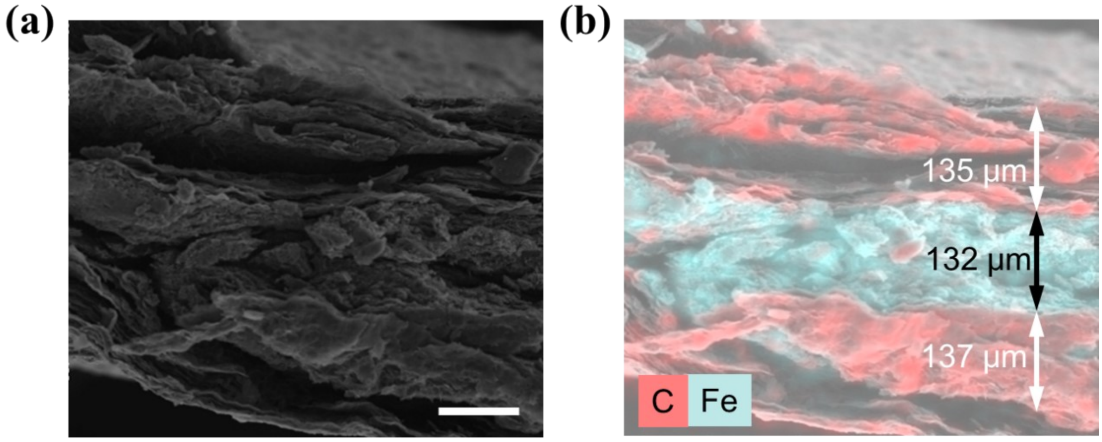

Figure S15. (a) Cross-sectional SEM image of multi-layered RGOD/Fe_2O_3@RGOD/RGOD, (b) along with its EDS mapping image and the thickness of each layer. (Inset) (Scale bar: 100 µm)

Table S1. Mechanical properties of GOD, GOD composites and RGOD composites.

	Elastic modulus (GPa)	**Hardness (MPa)**	**Vickers hardness (HV)**
GOD	2.42 ± 0.43	88 ± 13	8.12 ± 1.2
Fe_2O_3@CNT@GOD	2.76 ± 0.40	149 ± 20	13.8 ± 1.8
RuO_2@CNT@GOD	3.40 ± 0.19	178 ± 14	16.5 ± 1.3
Fe_2O_3@CNT@RGOD	14.3 ± 1.0	374 ± 39	34.6 ± 3.5
RuO_2@CNT@RGOD	15.3 ± 1.3	488 ± 41	41.5 ± 3.8

Table S2. Comparison of electrochemical performance of RuO_2@CNT@RGOD electrode with other high-density carbon materials including composite structures reported in the literature using a two-electrode system.

Materials	Density ($g\ cm^{-3}$)	C_v ($F\ cm^{-3}$) @ scan rate	E_v (Wh/L)	P_v (W/L)	Cycling stability	Electrolyte	Ref.
NCGH-40	1.35	351.8 @ 0.3 A/g 282.7 @ 10 A/g	12.2 8.4	101 3126.3	110.4% @ 10 A/g (1,000 cycles)	6M KOH	[1]
F-RGO-60	1.47	262.5 @ 0.1 A/g 200.2 @ 10 A/g	9.14 7.28	36.7 631	91.5% @ 5 A/g (6,000 cycles)	6M KOH	[2]
POGH	0.94	241.1 @ 0.5 A/g 221.3 @ 10 A/g	8.3 6.7	116.9 2,193	100.7% @ 10 A/g (10,000 cycles)	6M KOH	[3]
NFGH5	1.17	309.2 @ 0.3 A/g 231.9 @ 10 A/g	10.7 7.1	87.6 2,748	93.8% @ 10 A/g (10,000 cycles)	6M KOH	[4]
HOGH-140	1.16	377.8 @ 0.3 A/g 200.3 @ 10 A/g	13.1 9.7	86.9 2,777	99% @ 10 A/g (10,000 cycles)	6M KOH	[5]
SC-PPC	0.70	278.6 @ 0.5 A/g 175 @ 20 A/g	8.05 4.9	109.7 3310.3	96% at 10 A/g (10,000 cycles)	4M H_2SO_4	[6]
MPCN-800	0.85	318 @ 0.5 A/g 248 @ 20 A/g	8.67 6.97	110.5 4,505	96% at 10 A/g (30,000 cycles)	6M KOH	[7]
PCS	0.75	268 @ 1 A/g 218 @ 20 A/g	8.8 7.4	187.5 9,375	100% at 20 A/g (10,000 cycles)	6M KOH	[8]
PANi-NT-graphene	1.19	369.5 @ 1 A/g	8.21	2896.9	97.6% at 20 A/g (5,000 cycles)	1M H_2SO_4	[9]
NGCH-150	1.35	404.6 @ 0.3 A/g	14.0	~3250	93.8% @ 10 A/g (10,000 cycles)	6M KOH	[10]
prGO-CNT	1.50	250 @ 1 A/g 200 @ 10 A/g	8.2	4200	97% @ 10 A/g (5,000 cycles)	6M KOH	[11]
This work	**1.63**	**285 @ 0.5 A/g** **206 @ 20 A/g**	**9.90** **7.15**	**204** **8,119**	**93 % @ 10 A/g** **(10,000 cycles)**	**6M KOH**	

Table S3. Comparison of EMI SE performance of various polymer-free graphene composite materials fabricated using different methods, including process temperature and time, along with representative commercial shielding materials.

Materials	Thickness (mm)	Density (g cm^{-3})	Conductivity (S cm^{-1})	EMI SE (dB) @ Frequency (GHz)	Mixing process (Taken temp. and time)	Post-processing (Taken temp. and time)	Ref.
D-LIG/Ni	0.327	-	43.9	79 @ 8.2-12.4	Electrochemical deposition (RT, 30 min)	-	[12]
CNT-MLGEP	1.6	0.0089	1.18	47.5 @ 8.2-12.4	PECVD (800 °C, < 2 h)	Annealing (600 °C, 3h)	[13]
CNT-gGF	0.24	-	1.3*10^{4}	55 @ 5-22	Ball-milling (RT, 12 h)	Graphitization (2800 °C, 2h)	[14]
Graphene/CNTs	2	0.985	1819.17	75 @ 12.4-18	Ultra-sonication (RT, 50 min)	Graphitization (2800 °C, 2h)	[15]
Fe_3O_4/GN	0.20	0.78	50	24 @ 8.2-12.4	Hydrothermal reaction (180 °C, 10 h)	-	[16]
$NiFe_2O_4$/rGO	2	-	0.7	38.2 @ 10.8	Hydrothermal reaction (200 °C, 12 h)	-	[17]
Fe_3O_4@MWCNTs/RGO	0.6	0.108	5.076	45.9 @ 8.2-12.4	Stirring and dry (50 °C, 12h)	- Hydrothermal reaction (100 °C, 1h)	[18]
PGFs-*x*PFO	2.18	-		64.36 @ 2-18	MLD (150 °C, < 2 min)	Annealing (380 °C, 1h)	[19]
Graphene/Ag	0.8	-	0.032	28 @ 8.2-12.4	Stirring and heating (100 °C, 4.5h)	Thermal drying (50 °C, 24h)	[20]
f-Fe_3O_4-VCNTs@rGO	1	-	-	25 @ 8.2-12.4	Microwave method (RT, <5 min)	-	[21]
MRGO-MX Foam	15	0.0038	0.81	35 @ 8.2-12.4	Stirring and sonication (RT, ~30 min)	Thermal drying (90 °C, 12h)	[22]
Copper Foil	0.01	8.97	8.0*10^{5}	70 @ 8.2-12.4	-		[23]
Aluminum Foil	0.05	2.7	3.5*10^{5}	62.5 @ 8.2-12.4	-		[24]

Silver foil	0.01	10.49	$6.0*10^5$	58.49 @ 8.2-12.4	-		[24]
Carbon fabric	0.109	1.1	1351.35	47.11 @ 8.2-12.4	-		[24]
This work	**0.5**	**1.12**	**16.1**	**81.3 @ 8.2-12.4**	**Directly physical mixing (RT, 3-5 min)**	**Annealing (250 ℃, 1h)**	

References

1 Y. Zhang, K. Liu, X. Liu, W. Ma, S. Li, Q. Zhou, H. Pan and S. Fan, *Energy and Fuels*, 2022, **36**, 8506–8514.

2 C. Huang, A. Hu, Y. Li, H. Zhou, Y. Xu, Y. Zhang, S. Zhou, Q. Tang, C. Chen and X. Chen, *Nanoscale*, 2019, **11**, 16515–16522.

3 Y. Zhang, S. Fan, S. Li, Y. Song and G. Wen, *J. Mater. Sci.*, 2020, **55**, 12214–12231.

4 J. Chen, Q. Zhou, W. Ma, C. Wang, S. Fan and Y. Zhang, *J. Mater. Sci. Mater. Electron.*, 2024, **35**, 1–13.

5 S. Fan, L. Wei, X. Liu, W. Ma, C. Lou, J. Wang and Y. Zhang, *Int. J. Hydrogen Energy*, 2021, **46**, 39969–39982.

6 H. Gao, D. Zhang, H. Zhou, J. Wu, G. Xu, Z. Huang, M. Liu, J. Yang and D. Chen, *Appl. Surf. Sci.*, 2020, **534**, 147613.

7 X. Che, J. Yang, S. Liu, M. Wang, S. He and J. Qiu, *Ind. Eng. Chem. Res.*, 2022, **61**, 8908–8917.

8 S. Feng, Z. Liu, Q. Yu, Z. Zhuang, Q. Chen, S. Fu, L. Zhou and L. Mai, *ACS Appl. Mater. Interfaces*, 2019, **11**, 4011–4016.

9 M. Moussa, M. F. El-Kady, S. Abdel-Azeim, R. B. Kaner, P. Majewski and J. Ma, *Compos. Sci. Technol.*, 2018, **160**, 50–59.

10 Y. Zhang, L. Wei, X. Liu, W. Ma, C. Lou, J. Wang and S. Fan, *Int. J. Hydrogen Energy*, 2022, **47**, 33827–33838.

11 N. Díez, C. Botas, R. Mysyk, E. Goikolea, T. Rojo and D. Carriazo, *J. Mater. Chem. A*, 2018, **6**, 3667–3673.

12 J. Yin, J. Zhang, S. Zhang, C. Liu, X. Yu, L. Chen, Y. Song, S. Han, M. Xi, C. Zhang, N. Li and Z. Wang, *Chem. Eng. J.*, 2021, **421**, 129763.

13 Q. Song, F. Ye, X. Yin, W. Li, H. Li, Y. Liu, K. Li, K. Xie, X. Li, Q. Fu, L. Cheng, L. Zhang and B. Wei, *Adv. Mater.*, 2017, **29**, 1–8.

14 Y. Yu, F. Yang, X. Liu, D. Lu, T. Liu, Y. Li and Z. Wu, *Carbon N. Y.*, 2024, **228**, 119420.

15 H. Jia, Q. Q. Kong, X. Yang, L. J. Xie, G. H. Sun, L. L. Liang, J. P. Chen, D. Liu, Q. G. Guo and C. M. Chen, *Carbon N. Y.*, 2021, **171**, 329–340.

16 W. L. Song, X. T. Guan, L. Z. Fan, W. Q. Cao, C. Y. Wang, Q. L. Zhao and M. S. Cao, *J. Mater. Chem. A*, 2015, **3**, 2097–2107.

17 A. Kumar, A. K. Singh, M. Tomar, V. Gupta, P. Kumar and K. Singh, *Ceram. Int.*, 2020, **46**, 15473–15481.

18 J. Zhou, H. Tao, L. Xia, H. Zhao, Y. Wang, Y. Zhan and B. Yuan, *Compos. Commun.*, 2022, **32**, 101181.

19 S. Zhao, J. Yang, F. Duan, B. Zhang, Y. Liu, B. Zhang, C. Chen and Y. Qin, *J. Colloid Interface Sci.*, 2021, **598**, 45–55.

20 P. K. Sahoo, R. Aepuru, H. S. Panda and D. Bahadur, *Sci. Rep.*, 2015, **5**, 1–12.

21 R. Kumar, A. V. Alaferdov, R. K. Singh, A. K. Singh, J. Shah, R. K. Kotnala, K. Singh, Y. Suda and S. A. Moshkalev, *Compos. Part B Eng.*, 2019, **168**, 66–76.

22 Q. Chen, K. Zhang, L. Huang, Y. Li and Y. Yuan, *Adv. Eng. Mater.*, 2022, **24**, 1–12.

23 F. Shahzad, M. Alhabeb, C. B. Hatter, B. Anasori, S. M. Hong, C. M. Koo and Y. Gogotsi, *Science (80-.).*, 2016, **353**, 1137–1140.

24 H. Ji, R. Zhao, N. Zhang, C. Jin, X. Lu and C. Wang, *NPG Asia Mater.*, 2018, **10**, 749–760.